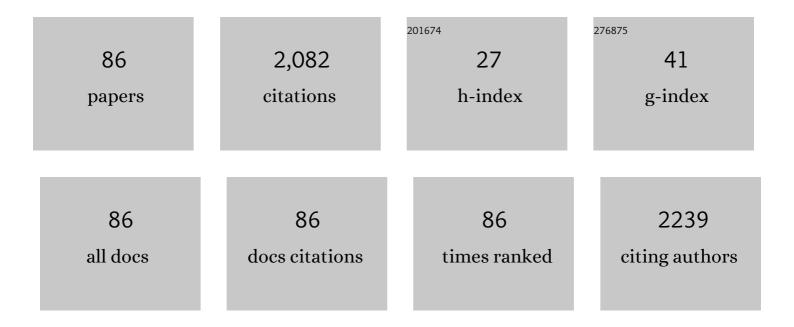
Zhifeng Wang

List of Publications by Year in descending order

Source: https://exaly.com/author-pdf/9038787/publications.pdf Version: 2024-02-01



#	Article	IF	CITATIONS
1	Defective ZnOx@porous carbon nanofiber network inducing dendrite-free zinc plating as zinc metal anode for high-performance aqueous rechargeable Zn/Na4Mn9O18 battery based on hybrid electrolyte. Journal of Power Sources, 2022, 518, 230761.	7.8	20
2	Microstructural Evolution and Mechanical Properties of Pure Aluminum upon Multi-Pass Caliber Rolling. Materials, 2022, 15, 1206.	2.9	2
3	Microstructure and discharge performance of Mg–6Al and Mg–6Al-0.5Er alloys. Materials Chemistry and Physics, 2022, 280, 125822.	4.0	11
4	Biodegradable Mg–Zn–Ca-Based Metallic Glasses. Materials, 2022, 15, 2172.	2.9	15
5	Self-standing porous Au/CuO nanowires with remarkably enhanced visible light absorption and photocatalytic performance. Applied Surface Science, 2022, 594, 153443.	6.1	13
6	Effect of 1wt%Zn Addition on Microstructure and Mechanical Properties of Mg-6Er Alloys under High Strain Rates. Metals, 2022, 12, 883.	2.3	2
7	Tailoring the microstructure and improving the discharge properties of dilute Mg-Sn-Mn-Ca alloy as anode for Mg-air battery through homogenization prior to extrusion. Journal of Materials Science and Technology, 2021, 60, 77-89.	10.7	57
8	NiCo2S4 nanoparticles embedded in nitrogen-doped carbon nanotubes networks as effective sulfur carriers for advanced Lithium–Sulfur batteries. Microporous and Mesoporous Materials, 2021, 316, 110924.	4.4	13
9	3D nanoporous Ni@NiO/metallic glass sandwich electrodes without corrosion cracks for flexible supercapacitor application. Applied Surface Science, 2021, 545, 149043.	6.1	24
10	A comparable study of Mg98.15Y1Zn0.85 sheets fabricated by twin-roll casting and direct-chill casting and related annealing behavior. Materials Science & Engineering A: Structural Materials: Properties, Microstructure and Processing, 2021, 815, 141316.	5.6	3
11	Flexible porous Ni(OH)2 nanopetals sandwiches for wearable non-enzyme glucose sensors. Applied Surface Science, 2021, 552, 149529.	6.1	30
12	Improving the cycling stability of three-dimensional nanoporous Ge anode by embedding Ag nanoparticles for high-performance lithium-ion battery. Journal of Colloid and Interface Science, 2021, 592, 103-115.	9.4	22
13	Controllable nanoporous copper synthesized by dealloying metallic glasses: New insights into the tuning pore structure and applications. Chemical Engineering Journal, 2021, 427, 130861.	12.7	6
14	Flexible Co(OH)2/NiOxHy@Ni hybrid electrodes for high energy density supercapacitors. Chemical Engineering Journal, 2021, 415, 128871.	12.7	55
15	Effect of the pre-homogenization on the precipitation behaviors, mechanical and corrosion properties of as-extruded Mg Y binary alloys. Materials Characterization, 2021, 178, 111307.	4.4	6
16	Effect of Solution Temperature on Corrosion Behavior of 7050 Alloy after Heat Treatment in 3.5% NaCl Solution. International Journal of Electrochemical Science, 2021, 16, 210939.	1.3	1
17	Flower-like Ni3S2 hollow microspheres as superior sulfur hosts for lithium-sulfur batteries. Microporous and Mesoporous Materials, 2021, 326, 111355.	4.4	12
18	Sn modified nanoporous Ge for improved lithium storage performance. Journal of Colloid and Interface Science, 2021, 602, 563-572.	9.4	23

#	Article	IF	CITATIONS
19	Performances of Al-xLi alloy anodes for Al-air batteries in alkaline electrolyte. Journal of Alloys and Compounds, 2021, 889, 161677.	5.5	9
20	Synthesis of Si/Fe2O3-Anchored rGO Frameworks as High-Performance Anodes for Li-Ion Batteries. International Journal of Molecular Sciences, 2021, 22, 11041.	4.1	9
21	Ag particles modified CuxO (x = 1, 2) nanowires on nanoporous Cu-Ag bimetal network for antibacterial applications. Materials Letters, 2020, 258, 126823.	2.6	14
22	Discharge Behavior of Mg–Sn–Zn–Ag Alloys with Different Sn Contents as Anodes for Mg-air Batteries. Journal of the Electrochemical Society, 2020, 167, 020501.	2.9	42
23	Flexible integrated metallic glass-based sandwich electrodes for high-performance wearable all-solid-state supercapacitors. Applied Materials Today, 2020, 19, 100539.	4.3	45
24	Bimodal nanoporous NiO@Ni–Si network prepared by dealloying method for stable Li-ion storage. Journal of Power Sources, 2020, 449, 227550.	7.8	42
25	Formation and evolution of ultrathin Cu2O nanowires on NPC ribbon by anodizing for photocatalytic degradation. Applied Surface Science, 2020, 506, 144819.	6.1	27
26	Improving the Cycling Stability of Fe3O4/NiO Anode for Lithium Ion Battery by Constructing Novel Bimodal Nanoporous Urchin Network. Nanomaterials, 2020, 10, 1890.	4.1	7
27	Porous Si/Fe2O3 Dual Network Anode for Lithium–Ion Battery Application. Nanomaterials, 2020, 10, 2331.	4.1	11
28	Dual network porous Si/Al9FeSi3/Fe2O3 composite for high performance Li-ion battery anode. Electrochimica Acta, 2020, 358, 136936.	5.2	11
29	Effect of Deformation and Heat Treatment on Pitting Corrosion Behavior of 7050 Al Alloy. International Journal of Electrochemical Science, 2020, , 7531-7544.	1.3	2
30	Stearic Acid Coated MgO Nanoplate Arrays as Effective Hydrophobic Films for Improving Corrosion Resistance of Mg-Based Metallic Glasses. Nanomaterials, 2020, 10, 947.	4.1	6
31	Microstructure and Corrosion behavior of Friction Stir-Welded AZ31 alloy. International Journal of Electrochemical Science, 2020, , 1058-1071.	1.3	3
32	AlF3 microrods modified nanoporous Ge/Ag anodes fabricated by one-step dealloying strategy for stable lithium storage. Materials Letters, 2020, 276, 128254.	2.6	7
33	Discharge properties of low-alloyed Mg–Bi–Ca alloys as anode materials for Mg–air batteries: Influence of Ca alloying. Journal of Alloys and Compounds, 2020, 823, 153779.	5.5	52
34	Flexible Free-Standing CuxO/Ag2O (x = 1, 2) Nanowires Integrated with Nanoporous Cu-Ag Network Composite for Glucose Sensing. Nanomaterials, 2020, 10, 357.	4.1	4
35	Microstructure, Mechanical and Corrosion Properties of Mg-1.61Al-1.76Ca Alloy under Different Extrusion Temperatures. Journal of Materials Engineering and Performance, 2020, 29, 672-680.	2.5	6
36	Hierarchically Porous Carbon Derived from Biomass Reed Flowers as Highly Stable Li-Ion Battery Anode. Nanomaterials, 2020, 10, 346.	4.1	24

#	Article	IF	CITATIONS
37	High specific surface area bimodal porous carbon derived from biomass reed flowers for high performance lithium-sulfur batteries. Journal of Colloid and Interface Science, 2020, 569, 22-33.	9.4	103
38	Dual-network nanoporous NiFe2O4/NiO composites for high performance Li-ion battery anodes. Chemical Engineering Journal, 2020, 388, 124207.	12.7	54
39	Porous CuxO/Ag2O (xÂ=Â1, 2) nanowires anodized on nanoporous Cu-Ag bimetal network as a self-supported flexible electrode for glucose sensing. Applied Surface Science, 2020, 515, 146062.	6.1	34
40	Hierarchical nanoporous Pd ₁ Ag ₁ alloy enables efficient electrocatalytic nitrogen reduction under ambient conditions. Chemical Communications, 2019, 55, 10108-10111.	4.1	28
41	Chemical-dealloying to fabricate nonconductive interlayers for high-loading lithium sulfur batteries. Journal of Alloys and Compounds, 2019, 806, 881-888.	5.5	16
42	Facile Preparation of Inverse Nanoporous Cr ₂ O ₃ /Cu Catalysts for Reverse Waterâ€Gas Shift Reaction. ChemCatChem, 2019, 11, 5439-5443.	3.7	7
43	A Ni(OH) ₂ nanopetals network for high-performance supercapacitors synthesized by immersing Ni nanofoam in water. Beilstein Journal of Nanotechnology, 2019, 10, 281-293.	2.8	22
44	Nanoporous GeO2/Cu/Cu2O network synthesized by dealloying method for stable Li-ion storage. Electrochimica Acta, 2019, 300, 363-372.	5.2	28
45	Nanoporous Cu@Cu ₂ O hybrid arrays enable photo-assisted supercapacitor with enhanced capacities. Journal of Materials Chemistry A, 2019, 7, 15691-15697.	10.3	66
46	Surface Morphologies and Mechanical Properties of Mg-Zn-Ca Amorphous Alloys under Chemistry-Mechanics Interactive Environments. Metals, 2019, 9, 327.	2.3	5
47	Nanoporous Quasi-High-Entropy Alloy Microspheres. Metals, 2019, 9, 345.	2.3	11
48	AZ61 and AZ61-La Alloys as Anodes for Mg-Air Battery. Journal of Materials Engineering and Performance, 2019, 28, 2006-2016.	2.5	39
49	Ultrafine Cu2O/CuO nanosheet arrays integrated with NPC/BMG composite rod for photocatalytic degradation. Applied Surface Science, 2019, 483, 285-293.	6.1	36
50	Tailoring nanoporous structures of Ge anodes for stable potassium-ion batteries. Electrochemistry Communications, 2019, 101, 68-72.	4.7	67
51	Bimodal nanoporous Pd3Cu1 alloy with restrained hydrogen evolution for stable and high yield electrochemical nitrogen reduction. Nano Energy, 2019, 58, 834-841.	16.0	145
52	Flexible NiO micro-rods/nanoporous Ni/metallic glass electrode with sandwich structure for high performance supercapacitors. Electrochimica Acta, 2019, 297, 767-777.	5.2	64
53	Synergetic enhancement of the electronic/ionic conductivity of a Li-ion battery by fabrication of a carbon-coated nanoporous SnOxSb alloy anode. Nanoscale, 2018, 10, 7605-7611.	5.6	9
54	Facile fabrication of CuS microflower as a highly durable sodium-ion battery anode. Inorganic Chemistry Frontiers, 2018, 5, 1045-1052.	6.0	52

#	Article	IF	CITATIONS
55	Porous TiO2/Fe2O3 nanoplate composites prepared by de-alloying method for Li-ion batteries. Materials Letters, 2018, 211, 254-257.	2.6	23
56	Three-dimensional electrode with conductive Cu framework for stable and fast Li-ion storage. Energy Storage Materials, 2018, 11, 83-90.	18.0	32
57	Facile fabrication of polyether sulfone (PES) protecting layer on Cu foil for stable Li metal anode. Electrochimica Acta, 2018, 260, 407-412.	5.2	19
58	Preparation and Electrochemical Properties of Pomegranate-Shaped Fe2O3/C Anodes for Li-ion Batteries. Nanoscale Research Letters, 2018, 13, 344.	5.7	10
59	Improved Discharge Performance of Mg-6Al-7Pb Alloy by Microalloying with Ce. International Journal of Electrochemical Science, 2018, 13, 10325-10338.	1.3	17
60	Effects of Ag, Nd, and Yb on the Microstructures and Mechanical Properties of Mg‒Zn‒Ca Metallic Glasses. Metals, 2018, 8, 856.	2.3	7
61	Stable nanoporous Sn/SnO2 composites for efficient electroreduction of CO2 to formate over wide potential range. Applied Materials Today, 2018, 13, 135-143.	4.3	58
62	Mn3O4 Octahedral Microparticles Prepared by Facile Dealloying Process as Efficient Sulfur Hosts for Lithium/Sulfur Batteries. Metals, 2018, 8, 515.	2.3	3
63	Chemical Dealloying Synthesis of CuS Nanowire-on-Nanoplate Network as Anode Materials for Li-Ion Batteries. Metals, 2018, 8, 252.	2.3	28
64	Mechanical Properties and Degradation Behavior of Mg(100â^'7x)Zn6xYx(x = 0.2, 0.4, 0.6, 0.8) Alloys. Metals, 2018, 8, 261.	2.3	7
65	Yucca fern shaped CuO nanowires on Cu foam for remitting capacity fading of Li-ion battery anodes. Scientific Reports, 2018, 8, 6530.	3.3	56
66	Improved sodium-ion storage properties by fabricating nanoporous CuSn alloy architecture. RSC Advances, 2017, 7, 29458-29463.	3.6	14
67	CoFe2O4 nanoplates synthesized by dealloying method as high performance Li-ion battery anodes. Electrochimica Acta, 2017, 252, 295-305.	5.2	63
68	The effect of an external magnetic field on the dealloying process of the Ni–Al alloy in alkaline solution. Physical Chemistry Chemical Physics, 2017, 19, 18167-18171.	2.8	10
69	Controlling the Mechanical Properties of Bulk Metallic Glasses by Superficial Dealloyed Layer. Nanomaterials, 2017, 7, 352.	4.1	9
70	One-step synthesis of CuO@brass foil by dealloying method for low-cost flexible supercapacitor electrodes. Journal of Materials Science: Materials in Electronics, 2016, 27, 9206-9215.	2.2	23
71	Hierarchical nanoporous metal/BMG composite rods with excellent mechanical properties. Intermetallics, 2016, 77, 1-5.	3.9	9
72	Novel bioactive Fe-based metallic glasses with excellent apatite-forming ability. Materials Science and Engineering C, 2016, 69, 513-521.	7.3	27

#	Article	IF	CITATIONS
73	Crystalline Cu-silicide stabilizes the performance of a high capacity Si-based Li-ion battery anode. Journal of Materials Chemistry A, 2016, 4, 19140-19146.	10.3	37
74	Microstructure and Mechanical Properties of AA1235 Aluminum Foil Stocks Produced Directly from Electrolytic Aluminum Melt. Metallurgical and Materials Transactions B: Process Metallurgy and Materials Processing Science, 2016, 47, 731-739.	2.1	1
75	Dealloying of Cu-Based Metallic Glasses in Acidic Solutions: Products and Energy Storage Applications. Nanomaterials, 2015, 5, 697-721.	4.1	28
76	Fabrication and new electrochemical properties of nanoporous Cu by dealloying amorphous Cu–Hf–Al alloys. Intermetallics, 2015, 56, 48-55.	3.9	48
77	Tailored Dealloying Products of Cu-based Metallic Glasses in Hydrochloric Acid Solutions. Materials Research, 2014, 17, 1003-1009.	1.3	10
78	Synthesis of Cu xO(x = 1,2)/amorphous compounds by dealloying and spontaneous oxidation method. Materials Research, 2014, 17, 33-37.	1.3	17
79	Corrosion behavior of closed-cell AZ31 Mg alloy foam in NaCl aqueous solutions. Corrosion Science, 2014, 80, 247-256.	6.6	17
80	Tunable Nanocrystals Fabricated by Free Dealloying of Amorphous Ribbons. Journal of Nanomaterials, 2012, 2012, 1-6.	2.7	2
81	Direct Preparation of Nano-Quasicrystals via a Water-Cooled Wedge-Shaped Copper Mould. Journal of Nanomaterials, 2012, 2012, 1-6.	2.7	3
82	Fabrication and corrosion resistance of Mg-Zn-Y-based nano-quasicrystals alloys. Materials Research, 2012, 15, 51-56.	1.3	4
83	The analysis of residual stress in glass-to-metal seals for solar receiver tube. Materials & Design, 2010, 31, 1813-1820.	5.1	37
84	Dispersion of carbon nanotubes in hydroxyapatite powder by in situ chemical vapor deposition. Materials Science and Engineering B: Solid-State Materials for Advanced Technology, 2010, 166, 19-23.	3.5	24
85	Effect of Titanium, Antimony, Cerium and Carbon Nanotubes on the Morphology and Microhardness of Mg-based Icosahedral Quasicrystal Phase. Journal of Materials Science and Technology, 2010, 26, 27-32.	10.7	15

86 Mg-Based Quasicrystals. , 0, , .

2